Supplementary Material

Flux-Assisted Synthesis of Bismuth Nanoparticles Decorated Carbon Nitride for Efficient Photocatalytic Degradation of Endocrine Disrupting Compound

Bin Zheng[a], Wu Cui[a], Fengting He[a], Yang Zhang[a], Shuling Wang[a], Yangming Lu[a], Chaocheng Zhao[a,], Jinqiang Zhang[b], Xiaoguang Duan[b], Hongqi Sun[c], Shuaijun Wang[d,*]*

[a] State Key Laboratory of Petroleum Pollution Control, China University of Petroleum (East China), 66 West Changjiang Road, Qingdao 266580, PR China

[b] School of Chemical Engineering and Advanced Materials, The University of Adelaide, North Terrace, Adelaide, SA 5005, Australia

[c] School of Science, Edith Cowan University, 270 Joondalup Drive, Joondalup, WA 6027, Australia

[d] School of Energy and Power Engineering, Jiangsu University, Zhenjiang 212013, P.R. China

*Corresponding Authors

E-mail: zhaochch@upc.edu.cn(C. Zhao); shuaijunwang@ujs.edu.cn(S. Wang)

Structural characterization

The micro morphology was characterized by field emission scanning electron microscope (SEM: JEOL JSM-7900F). The internal structure and element composition were characterized by transmission electron microscope (TEM: JEOL JEM-2100). Bruker D8 advance powder X-ray diffractometer (Cu Kα Radiation, λ = 1.5418 Å) was analyzed by XRD and Fourier transform infrared (FTIR) was analyzed by Nicolet Nexus 670 infrared spectrometer (400 – 4000 cm^{-1}). The photoluminescence (PL) spectrum was measured with Hitachi F-4600 luminescent spectrophotometer. Electron paramagnetic resonance (EPR) spectra was measured by Bruker A300 spectrometer; Electrochemical impedance spectroscopy (EIS) and transient photocurrent were measured on an electrochemical workstation with three electrode system (CHI-660B, China), using 0.1 M Na_2SO_4 aqueous solution as electrolyte, conductive glass (FTO) with reactive active area of 1 cm^2 as working electrode, platinum wire as counter electrode and Ag/AgCl (saturated KCl) as reference electrode; Steady-state/time-resolved PL emission spectra (375 nm excitation) were measured at room temperature using Edinburgh FLS1000 fluorescence spectrometer. X-ray photoelectron spectroscopy (XPS) analysis was performed with Thermo ESCALAB 250 instrument, C1s was set to 284.8 eV, and the binding energy was calibrated. Ultraviolet visible diffuse reflectance spectrum (UV-Vis DRS) was measured by universal analysis TU-1901 ultraviolet visible spectrophotometer with $BaSO_4$ as reflectance standard. ICP-OES plasma emission spectrometer Aglient 5110 was used to test ICPOES.

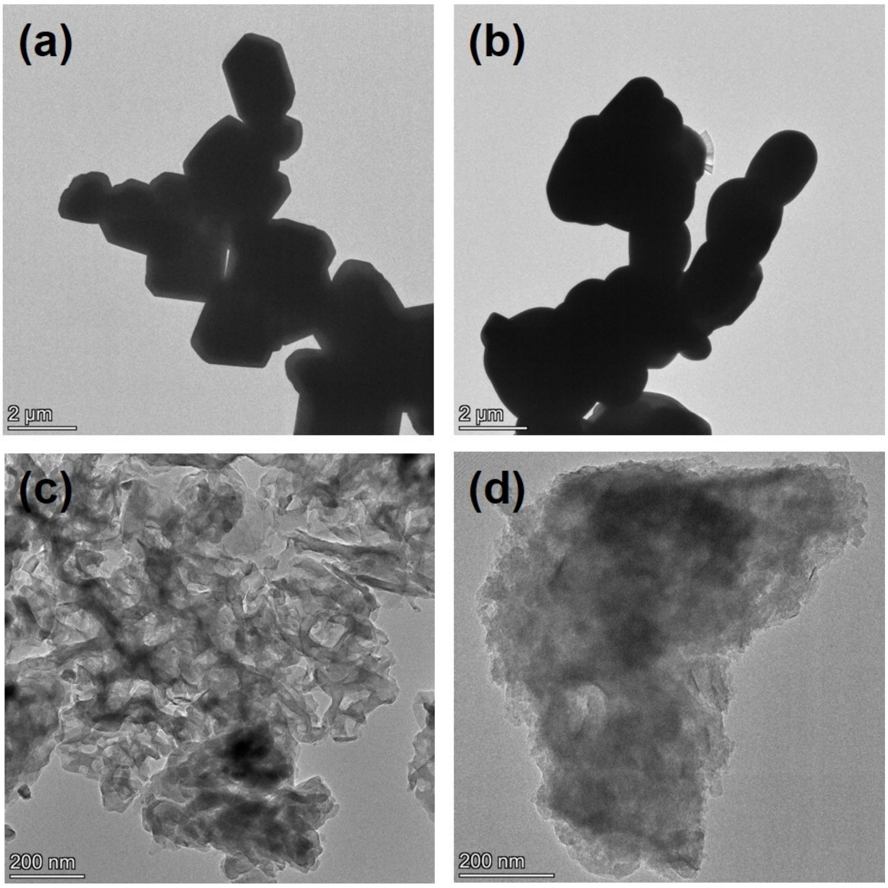

Fig. S1. TEM images of $BiVO_4$ (a), $cBiVO_4$ (b), BiCN-15(c) and BiCCN-15(d).

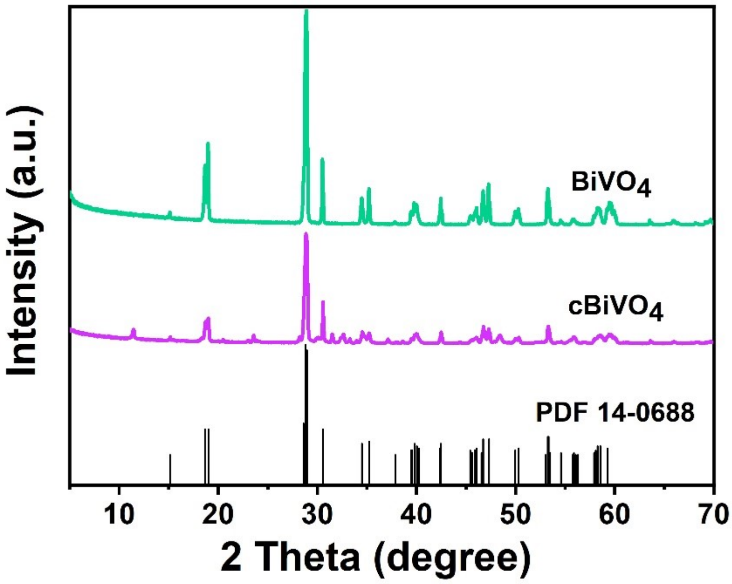

Fig. S2. XRD of $BiVO_4$ and $cBiVO_4$.

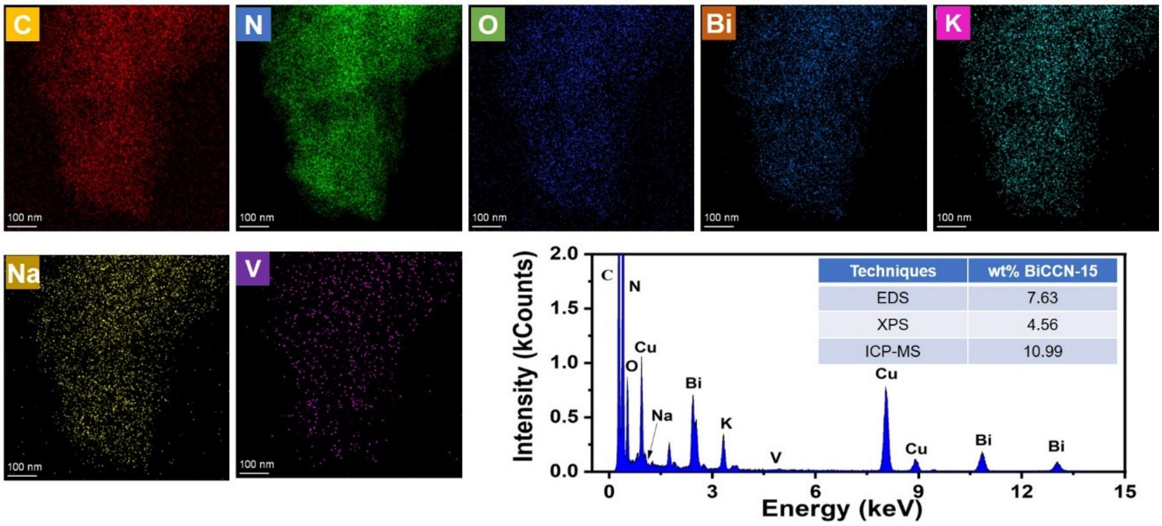

Fig. S3. EDS mapping of BiCCN-15 composite

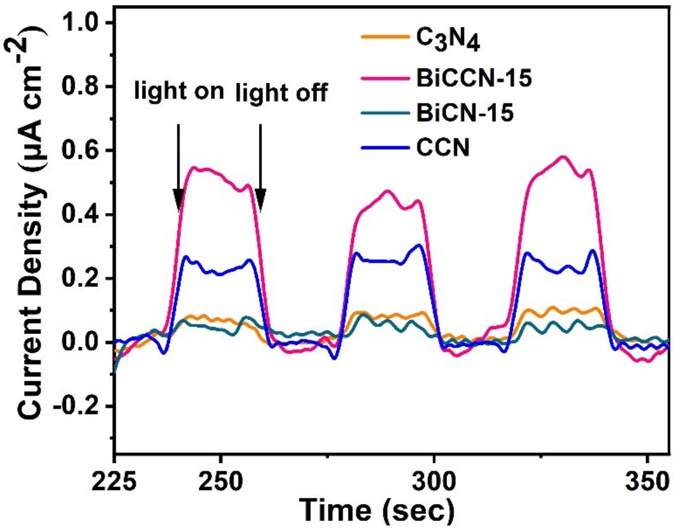

Fig. S4. Transient photocurrent responses plots of the as-prepared photocatalysts

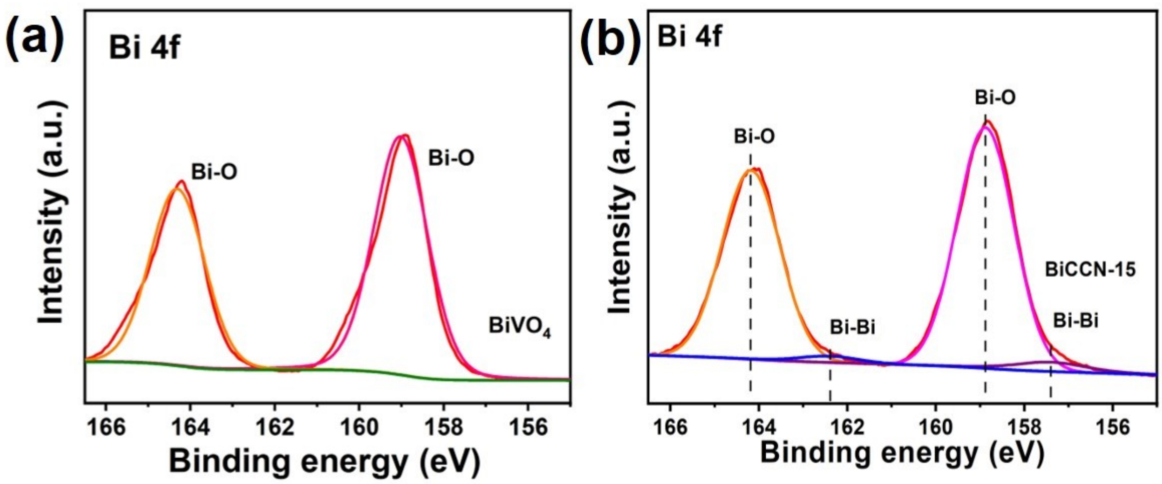

Fig. S5. Bi 4f spectral analysis of (a) $BiVO_4$ and (b) BiCCN-15

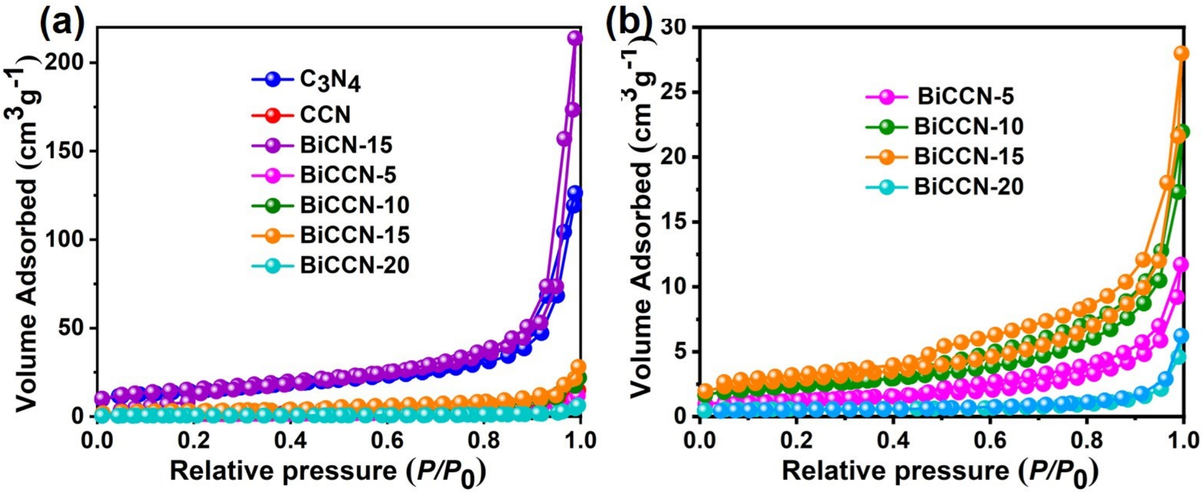

Fig. S6. N_2 adsorption and desorption curves of as-prepared samples

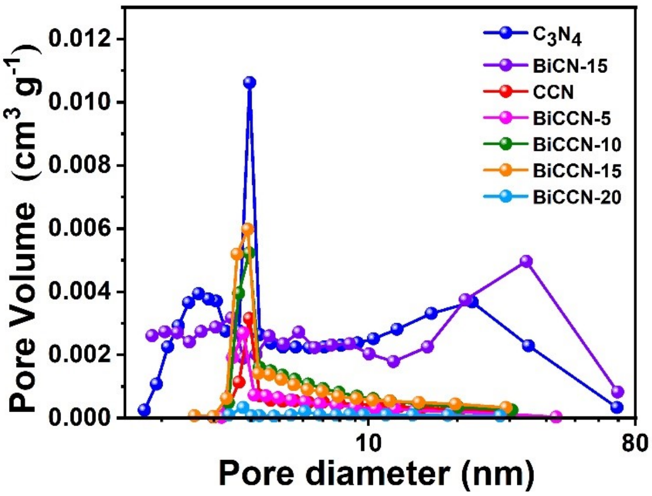

Fig. S7. Pore size distribution of prepared samples

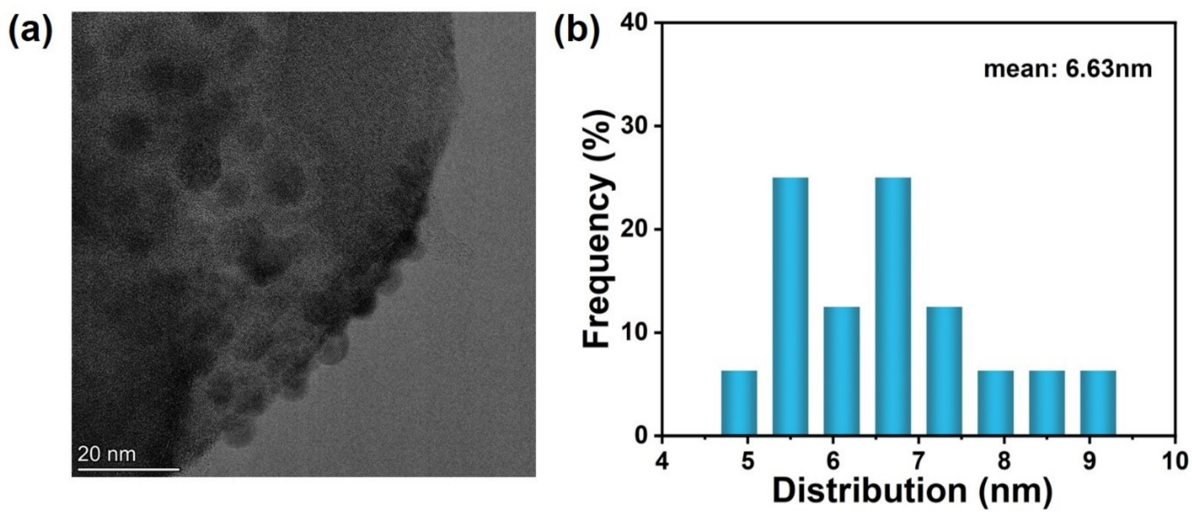

Fig. S8. HRTEM (a) and Bi NPs particle size distribution diagram of BiCCN-15

Table S1. Textural properties of the prepared samples.

Samples	S_{BET} ($m^2\ g^{-1}$)	Pore size (nm)	Pore volume ($cm^3\ g^{-1}$)
C_3N_4	50.83	17.19	0.19
CCN	4.76	11.07	0.02
BiCN-15	54.45	24.32	0.32
BiCCN-5	4.72	13.33	0.02
BiCCN-10	8.38	8.58	0.03
BiCCN-15	10.14	10.08	0.03
BiCCN-20	2.25	14.04	0.01

Table S2. The surface atomic ratios of all elements measured using XPS

Sample	%C (at)	%N (at)	%O (at)	%Cl (at)	%Na (at)	%K (at)	%Bi (at)	%V (at)
C_3N_4	41.8	57.29	0.91	0	0	0	0	0
CCN	44.64	44.69	4.66	0.14	2.43	3.44	0	0
BiCN-15	40.4	55.61	3.09	0	0	0	0.9	0
BiCCN-15	73.83	12.17	12.69	0.06	0.45	0.39	0.3	0.1

Table S3. Comparison of BPA degradation rates between BiCCN-15 and literature reported C_3N_4 photocatalysts

Photocatalysts	Catalyst (g/L)	Light source Xe lamp/W	Pseudo-first-order rate constant (min^{-1})		Enhanced factor over reference catalyst	References
			Bulk g-C_3N_4	Composite catalyst		
BiCCN-15	0.5	300W (λ>420 nm)	~2.1×10^{-3}	~55.3×10^{-3}	26.3	This work
Carbon-vacancy-modified g-C_3N_4	0.3	350W (λ>420 nm)	~3.4×10^{-3}	~5.6×10^{-3}	1.65	1
C-doping and defects co-modified g-C_3N_4	0.5	300W (λ≥400 nm)	~3.1×10^{-3}	~26.9×10^{-3}	8.68	2
Novel carbon and defects co-modified g-C_3N_4	0.2	300W (λ>420 nm)	~2.7×10^{-3}	~61.4×10^{-3}	22.7	3
onion-like carbon modified ultrathin g-C_3N_4	1	300W (λ>420 nm)	~6.7×10^{-3}	~38×10^{-3}	5.7	4
Ag-decorated S-doped g-C_3N_4	0.6	155W (λ = 280–630 nm)	~3.3×10^{-3}	~11.5×10^{-3}	3.5	5
Surface amorphous carbon doping of g-C_3N_4	0.3	300W (λ≥420 nm)	~3.8×10^{-3}	~50.7×10^{-3}	13.3	6
metal free 2D g-C_3N_4	0.5	300W	~11.3×10^{-3}	~45.0×10^{-3}	4.0	7
carbon and oxygen dual-doped g-C_3N_4	0.4	500W (λ>420 nm)	~18.5×10^{-3}	~86.3×10^{-3}	4.7	8
Oxygen doped g-C_3N_4	0.2	—	~1.1×10^{-3}	~32.0×10^{-3}	19.1	9
g-C_3N_4 nanosheets/PS	0.5	150 W (λ>400 nm)	~2.8×10^{-3}	~14.0×10^{-3}	5.0	10

References

1 X. Liang, G. Wang, X. Dong, G. Wang, H. Ma and X. Zhang, Graphitic carbon nitride with carbon vacancies for photocatalytic degradation of bisphenol A, *ACS Appl. Nano Mater.*, 2019,2(1), 517-524.

2 X. He, L. Lei, J. Wen, Y. Zhao, L. Cui and G. Wu, One-pot synthesis of C-doping and defects co-modified g-C_3N_4 for enhanced visible-light photocatalytic degradation of bisphenol A, *J. Environ. Chem. Eng.*, 2022,10(1), 106911.

3 M. Wu, X. He, B. Jing, T. Wang, C. Wang, Y. Qin, Z. Ao, S. Wang and T. An, Novel carbon and defects co-modified g-C_3N_4 for highly efficient photocatalytic degradation of bisphenol A under visible light, *J. Hazard. Mater.*, 2020,384, 121323.

4 Y. Wang, H. Cai, F. Qian, Y. Li, J. Yu, X. Yang, M. Bao and X. Li, Facile one-step synthesis of onion-like carbon modified ultrathin g-C_3N_4 2D nanosheets with enhanced visible-light photocatalytic performance, *J. Colloid Interface Sci.*, 2019,533, 47-58.

5 W.-D. Oh, L.-W. Lok, A. Veksha, A. Giannis and T.-T. Lim, Enhanced photocatalytic degradation of bisphenol A with Ag-decorated S-doped g-C_3N_4 under solar irradiation: Performance and mechanistic studies, *Chem. Eng. J.*, 2018,333, 739-749.

6 F. Ge, Y. Xu, Y. Zhou, D. Tian, S. Huang, M. Xie, H. Xu and H. Li, Surface amorphous carbon doping of carbon nitride for efficient acceleration of electron transfer to boost photocatalytic activities, *Appl. Surf. Sci.*, 2020,507, 145145.

7 R. S. Sahu, Y.-h. Shih and W.-L. Chen, New insights of metal free 2D graphitic carbon nitride for photocatalytic degradation of bisphenol A, *J. Hazard. Mater.*, 2021,402, 123509.

8 J. Gu, H. Chen, F. Jiang and X. Wang, Visible light photocatalytic mineralization of bisphenol A by carbon and oxygen dual-doped graphitic carbon nitride, *J. Colloid Interface Sci.*, 2019,540, 97-106.

9 X. Long, C. Feng, S. Yang, D. Ding, J. Feng, M. Liu, Y. Chen, J. Tan, X. Peng, J. Shi and R. Chen, Oxygen doped graphitic carbon nitride with regulatable local electron density and band structure for improved photocatalytic degradation of bisphenol A, *Chem. Eng. J.*, 2022,435, 134835.

10 B. Liu, M. Qiao, Y. Wang, L. Wang, Y. Gong, T. Guo and X. Zhao, Persulfate enhanced photocatalytic degradation of bisphenol A by g-C_3N_4 nanosheets under visible light irradiation, *Chemosphere*, 2017,189, 115-122.